Developmental and Regional Changes in the Neurochemical Profile of the Rat Brain Determined by In Vivo ^{1}H NMR Spectroscopy

Ivan Tkáč,[1*] Raghavendra Rao,[2,4] Michael K. Georgieff,[2–4] and Rolf Gruetter[1,4,5]

Sixteen metabolites were quantified from 11–24 μl volumes in three different brain regions (hippocampus, striatum, and cerebral cortex) during postnatal development. Rat pups from the same litter were repeatedly measured on postnatal days 7, 10, 14, 21, and 28 using a completely noninvasive and longitudinal study design. Metabolite quantification was based on ultra-short echo-time ^{1}H NMR spectroscopy at 9.4 T and LCModel processing. Most of the brain metabolites were quantified with Cramer-Rao lower bounds (CRLB) less than 20%, which corresponded to an estimated concentration error <0.2 μmol/g. Taurine and total creatine were quantified with CRLB ≤ 5% from all 114 processed spectra. The resulting high reliability and reproducibility revealed significant regional and age-related changes in metabolite concentrations. The most sensitive markers for developmental and regional variations between hippocampus, striatum, and cerebral cortex were N-acetylaspartate, *myo*-inositol, taurine, glutamate, and choline compounds. Absolute values of metabolite concentrations were in very good agreement with previously published in vitro results based on chromatographic measurements of brain extracts. The current data may serve as a reference for studies focused on developmental defects and pathologies using neonatal rat models. Magn Reson Med 50:24–32, 2003. © 2003 Wiley-Liss, Inc.

Key words: ^{1}H NMR spectroscopy; neonatal rat brain; development; quantification; high field

The late fetal and early neonatal periods in humans can be evaluated by MR techniques, which reveal that significant regional changes in brain structure (1), function (2), and neurochemistry (3) occur over time. The rat brain between postnatal days 7 and 28 (P7–P28) is an established model for studies of early human brain development, where the P7 animal corresponds neurodevelopmentally to the human fetus at ~34 weeks gestation and the P28 animal to a 2–3-year-old human infant (4). This rapid postnatal development is associated with substantial biochemical changes (5–7) that in the past were assessed using in vitro methods based on sacrificing the animals at different postnatal ages. Typically, extracts of the removed brains were analyzed by chromatographic methods or NMR spectroscopy (8–11). Noninvasive in vivo ^{1}H and ^{31}P NMR spectroscopy have been used as well for developmental studies of the rat brain. However, only concentration ratios of a limited number of metabolites such as N-acetylaspartate, choline, creatine, phosphocreatine, and phosphorylethanolamine (12–14) were measured. Furthermore, the spectra were taken from large volumes containing the majority of the brain tissue, without taking into account regional biochemical variations.

Recently, we have shown that at least 18 metabolites ("neurochemical profile") can be quantified noninvasively in adult rat brain using highly spectrally and spatially resolved ^{1}H NMR spectroscopy at 9.4 T, based on FASTMAP shimming (15,16), high-performance ultra-short echo-time localization (17), and LCModel spectral analysis (18). The purpose of the present study was to *comprehensively* measure the developmental changes of metabolite concentrations in three different regions of the neonatal rat brain using a completely noninvasive longitudinal study design. The hippocampus and the striatum were chosen because of their central roles in recognition and procedural memory functions, respectively, and the cerebral cortex was selected due to its involvement in higher executive functions. These areas are hypothesized to be selectively vulnerable to neonatal insults (19,20). The developing rat brain with its large range of metabolite concentration changes served as a suitable model to test and validate used spectroscopic technique and the method of quantification.

MATERIALS AND METHODS

Animals

Experiments were performed according to procedures approved by the Institutional Animal Care and Use Committee. Pregnant Sprague-Dawley dams were housed in the local animal facility to exactly determine the day of birth. The number of pups in a litter was randomly culled to eight soon after birth. The body weight of the rat pups increased with age (mean ± SD): 15 ± 2 g (P7), 23 ± 3 g (P10), 34 ± 3 g (P14), 56 ± 4 g (P21), 85 ± 6 g (P28). Spontaneously breathing rats were fixed in a chamber and anesthetized by flow of a gas mixture (N_2O:O_2 = 1:1) containing 1.5–2% isoflurane. The air temperature surrounding the rat chamber was maintained at 30°C by warm

[1]Center for Magnetic Resonance Research, University of Minnesota, Minneapolis, Minnesota.

[2]Department of Pediatrics, University of Minnesota, Minneapolis, Minnesota.

[3]Institute of Child Development, University of Minnesota, Minneapolis, Minnesota.

[4]Center for Neurobehavioral Development, University of Minnesota, Minneapolis, Minnesota.

[5]Department of Neuroscience, University of Minnesota, Minneapolis, Minnesota.

Grant sponsor: NICHD; Grant numbers: 1R29HD29421 (to M.K.G.); P30HD33692 (to R.R.); Grant sponsor: Center for MR research in part supported by the National Center for Regional Resources (NCRR); Grant number: P41RR08079-10; Grant sponsor: W.M. Keck Foundation.

*Correspondence to: Ivan Tkáč, Ph.D., Center for Magnetic Resonance Research, Department of Radiology, University of Minnesota, 2021 6th Street SE, Minneapolis, MN 55455. E-mail: ivan@cmrr.umn.edu

Received 5 December 2002; revised 12 February 2003; accepted 8 March 2003.

DOI 10.1002/mrm.10497
Published online in Wiley InterScience (www.interscience.wiley.com).

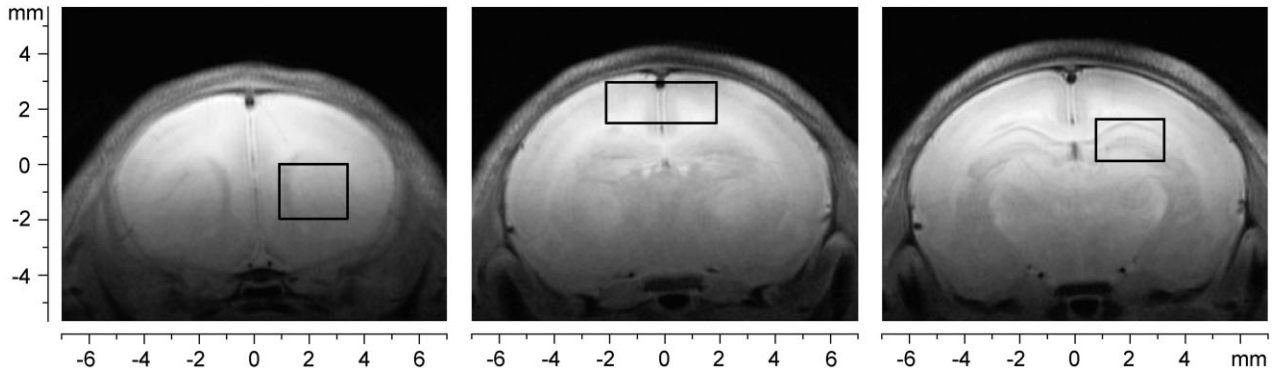

FIG. 1. RARE images of a rat brain (7) with the volumes of interest (VOI) centered in striatum, cortex, and hippocampus selected for NMR spectroscopy studies. ETL = 8, TE = 48 ms, matrix = 256 × 256, slice thickness = 1 mm.

water circulation and verified by a thermosensor. The duration of a study of a single animal did not exceed 100 min. The experiments were performed longitudinally, i.e., the rat pups were measured repeatedly over the first 4 postnatal weeks. Two litters were used to study the hippocampus, striatum, and cerebral cortex, resulting in 5–9 measurements per brain location per postnatal day. An additional litter was used to measure spectra from

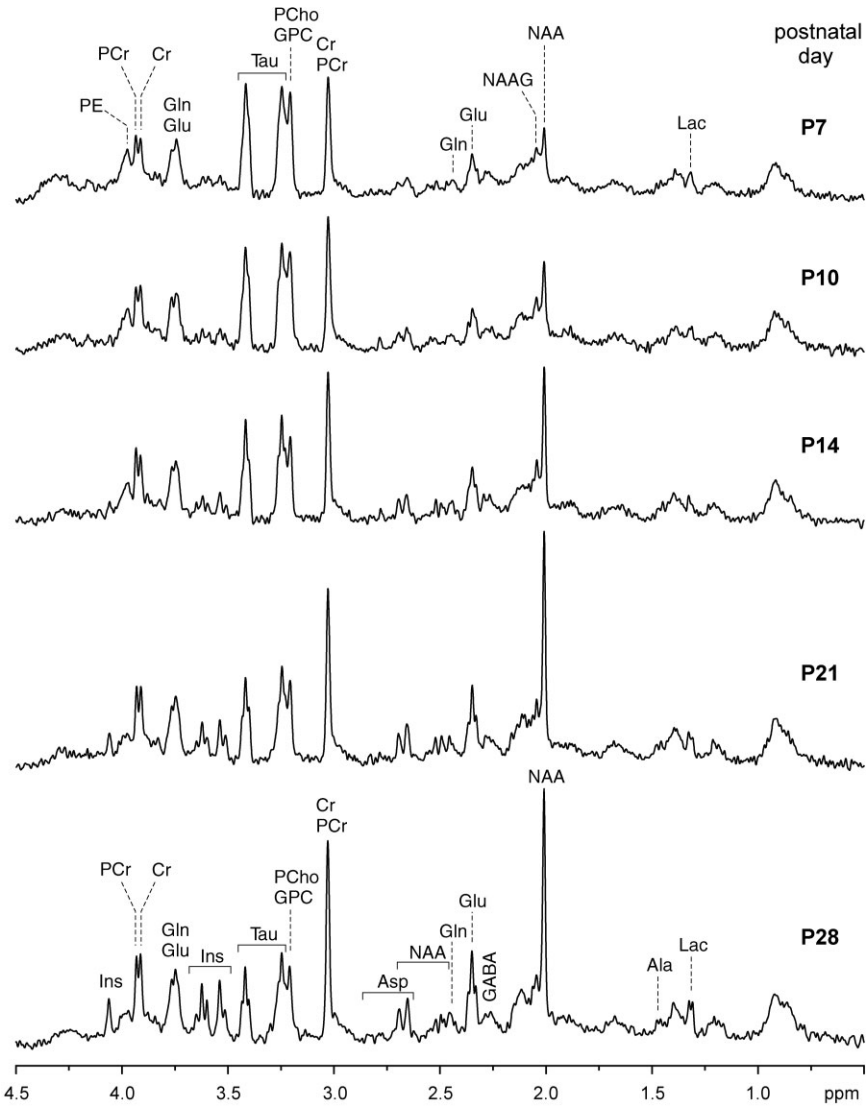

FIG. 2. In vivo ^{1}H NMR spectra of the developing rat hippocampus (P7–P28). STEAM, TE = 2 ms, TM = 20 ms, TR = 5 sec, NT = 320, VOI = 11–18 μl. Processing: Gaussian multiplication (gf = 0.12, gfs = 0.05), FT, and zero-order phase correction. No water signal removal or baseline corrections were applied.

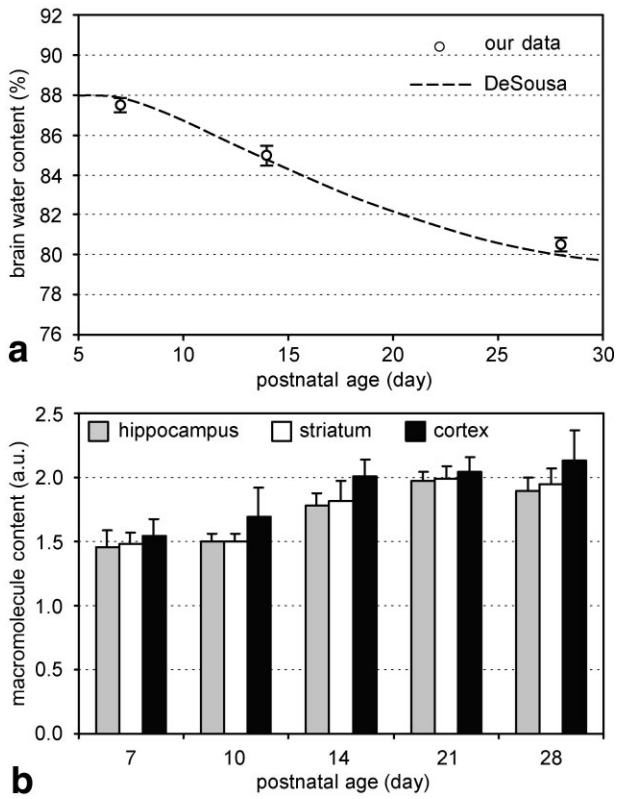

FIG. 3. **a:** Dependence of the brain water content on postnatal age. Comparison of our experimental data with the data published by De Souza and Dobbing (23). **b:** Macromolecule content in hippocampus, striatum, and cerebral cortex of the developing rat brain.

hippocampus only, resulting in 9–12 measurements per postnatal day in that brain region.

^{1}H NMR Spectroscopy

All experiments were performed on a 9.4 T/31cm magnet (Magnex Scientific, Abingdon, UK) equipped with an 11-cm gradient coil (300 mT/m, 500 μs) retrofitted with a strong custom-designed shim coil (Magnex Scientific) with second-order shim strengths up to 0.04 mT/cm^2. The magnet was interfaced to a Varian INOVA console (Varian, Palo Alto, CA). A quadrature transmit/receive surface RF coil with two geometrically decoupled single-turn coils with a 14 mm diameter each was used. All first- and second-order shim terms were adjusted for each volume of interest (VOI) based on a recently improved FASTMAP method using EPI readout (16). The water signal was efficiently suppressed by variable power RF pulses with optimized relaxation delays (VAPOR) (17). Localization was performed using ultra-short echo-time STEAM (TE = 2 ms, TM = 20 ms, TR = 5 sec) with asymmetric RF pulses combined with outer volume saturation (OVS) (17). The displacement error was minimized by using broadband RF pulses (13.5 kHz in STEAM, 35 kHz for OVS) combined with field gradients of 100–200 mT/m for slice selection. Data were acquired as a series of FIDs (consisting of 16 averages each) that were separately saved on a disk. The FIDs were individually corrected for frequency drift, then summed together and corrected for residual eddy current effects using reference water signal (21). ^{1}H NMR spectra were acquired from the VOIs centered in hippocampus, striatum, and cerebral cortex. The positions of VOIs were based on RARE images (echo train length (ETL) = 8, echo spacing 12 ms, TE = 48 ms, number of phase-encoding steps = 128, slice thickness = 1 mm, number of transients NT = 2, TR = 4 sec). The dimensions of VOIs were slightly increased with age, in particular for hippocampus, to minimize potential partial volume effects in the developing brain. In hippocampus the VOI ranged from 2.5 × 1.5 × 3.0 mm^3 to 3.0 × 2.0 × 3.0 mm^3, in striatum from 3.0 × 2.0 × 3.0 mm^2 to 3.0 × 2.0 × 4.0 mm^2, and in cortex from 4.0 × 1.5 × 3.0 mm^3 to 4.0 × 1.5 × 4.0 mm^3. Fully automatic shimming, RF power, and water suppression adjustment required less than 3 min per brain region. In conjunction with the increased sensitivity at 9.4 T, this allowed us to collect multislice images as well as spectra from all three different locations and sufficient S/N within 100 min.

Quantification

^{1}H NMR spectra were analyzed using LCModel (22) including a macromolecule spectrum in the database, according to previously described procedures (18). The unsuppressed water signal, corrected for age-dependent changes in brain water content, was used as an internal reference. The brain water content was measured on P7, P14, and P28 using the weight difference between freshly removed brain and its residue after lyophilization. The following 18 metabolites were quantified from each spectrum: alanine (Ala), aspartate (Asp), creatine (Cr), γ-aminobutyric acid (GABA), glucose (Glc), glutamate (Glu), glutamine (Gln), glutathione (GSH), glycerophosphorylcholine (GPC), phosphorylcholine (PCho), *myo*-inositol (Ins), lactate (Lac), N-acetylaspartate (NAA), N-acetylaspartylglutamate (NAAG), phosphocreatine (PCr), phosphorylethanolamine (PE), *scyllo*-inositol, and taurine (Tau).

Statistical Analysis

The SPSS software package (SPSS, Chicago, IL) was used for statistical analysis. The data for each metabolite were first tested for a normal distribution (Kolmogorov-Smirnov test) and then statistically analyzed by a multivariate analysis of variance (MANOVA) with post-hoc multiple comparison (Bonferroni). Finally, a Pearson correlation analysis was performed.

RESULTS

Typical locations and sizes of the VOIs centered in hippocampus, striatum, and cortex, which were selected for spectroscopic studies, are shown in Fig. 1. In vivo ^{1}H NMR spectra from these three brain regions were acquired on P7, P10, P14, P21, and P28. The ^{1}H NMR spectra of the developing rat hippocampus shown in Fig. 2 represent the spectral quality observed routinely throughout this study for this brain region. The increase of NAA, Glu, Ins, and total creatine (Cr + PCr) and the decrease of Tau and PE

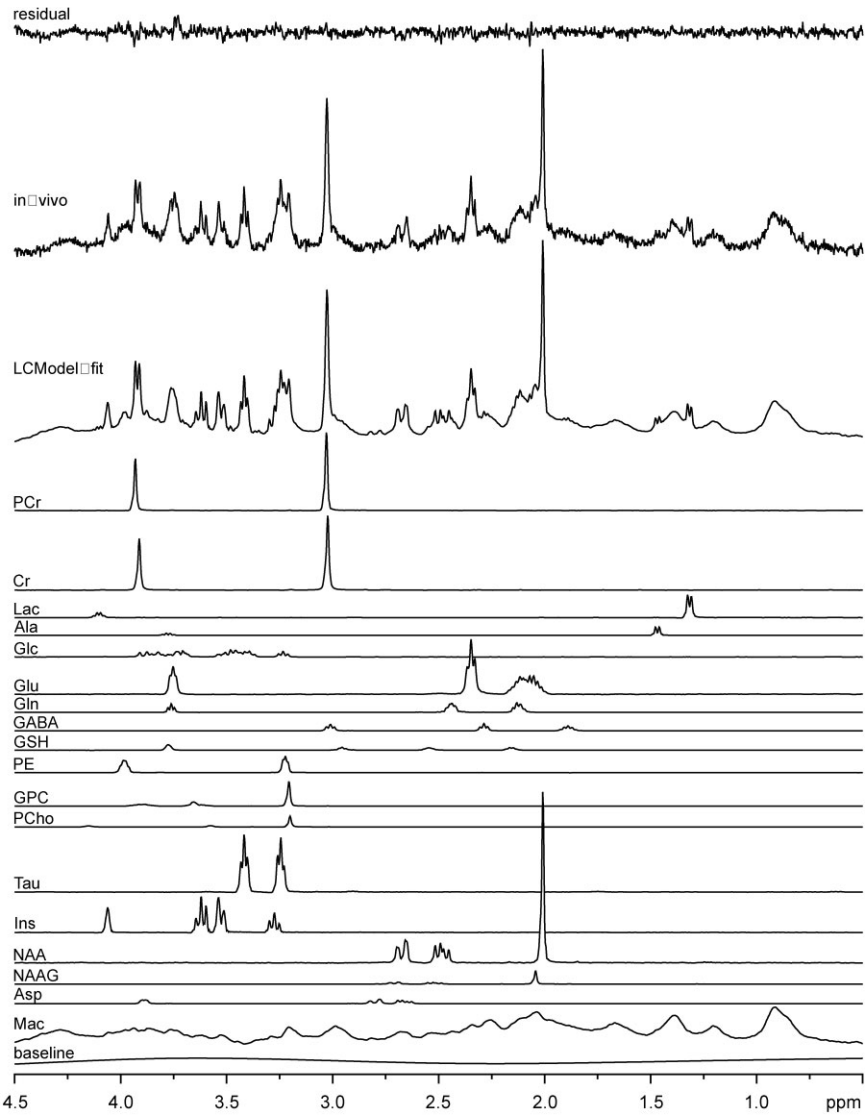

FIG. 4. LCModel fit of a ^{1}H NMR spectrum measured from rat hippocampus on postnatal day 28. In vivo spectrum (nonfiltered FT), fitted spectrum, residual, model solution spectra of brain metabolites, and the spectrum of fast-relaxing macromolecules (Mac).

during postnatal brain development (clearly visible in Fig. 2) were consistently observed in all three brain regions.

The unsuppressed water signal from the VOI was used for absolute metabolite quantification. Brain water contents measured on P7, P14, and P28 (Fig. 3a) were in very good agreement with previously published data (23). As in previous studies, a small but significant decrease in brain water content was observed during postnatal development. The macromolecule content, which was quantified from each spectrum as part of the LCModel analysis, was found to be highly reproducible in all age groups and in all three studied regions of the brain (coefficients of variation $<10\%$) and showed a modest increase of approximately 30% during postnatal development (Fig. 3b).

An experimentally measured spectrum from the hippocampus of a P28 rat was chosen as an example to illustrate the principle of LCModel analysis of short echo-time ^{1}H NMR spectra measured at 9.4 T. (Fig. 4). In this analysis, the in vivo spectrum of the brain was decomposed into 18 spectra of individual metabolites and the spectrum of fast relaxing macromolecules included in the LCModel database. The Cramer-Rao lower bounds (CRLB), which are the estimates of the precision of the fitted concentrations, were below 20% for most of the metabolites in all age groups and in all three studied regions of the brain. This corresponded to an estimated error of calculated concentration <0.2 μmol/g. Taurine and total Cr were quantified with CRLB $\leq 5\%$ from all 114 processed spectra. Only a few weakly represented metabolites, such as Ala, Asp, and NAAG, were quantified with CRLB exceeding 20% in some age groups. Finally, CRLB $> 20\%$ was found for Ins in P7 rats, where the Ins concentration was below 0.5 μmol/g. The results of the metabolite quantification in three different regions (hippocampus, striatum, and cerebral cortex) of the developing rat brain are summarized in Figs. 5 and 6. *Scyllo*-inositol, although included in the LCModel database, was not further analyzed because it was not detected in 50% of the processed spectra. In addition, the sum of PCho and GPC was used to evaluate the regional and developmental changes because of a strong cross-correlation between PCho and GPC that arises from the close spectral similarity (as illustrated in Fig. 4). The concentration of glucose was 4–5 μmol/g independent of age and brain location. The sum of Cr and PCr is

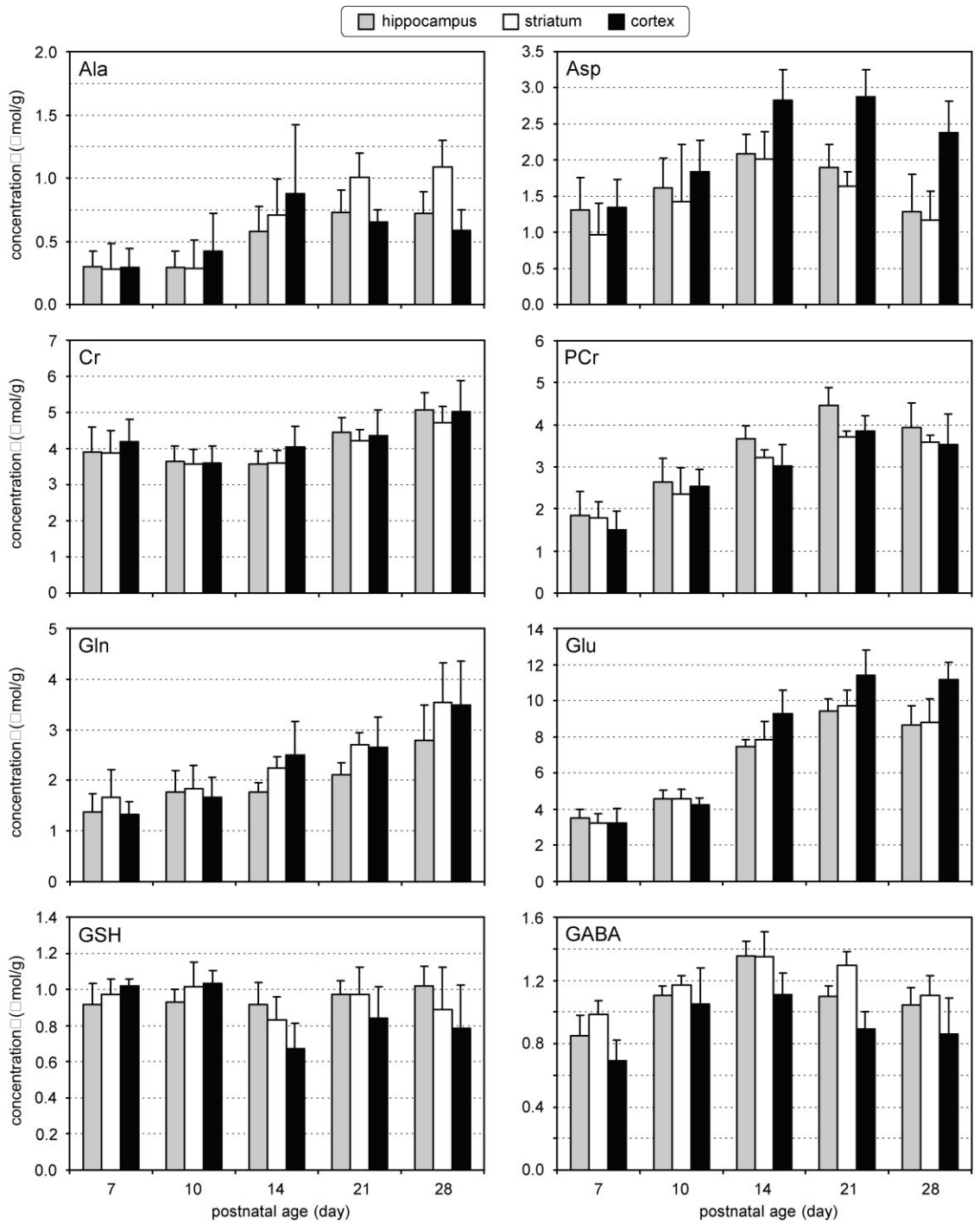

FIG. 5. Concentration of brain metabolites in hippocampus, striatum, and cerebral cortex in the developing rat brain (P7–P28). Error bars denote standard deviations.

also included in Fig. 6 for easier comparison with published data.

The statistical distribution of data for each metabolite in all three brain regions and all age groups was assessed to be normal using a Kolmogorov-Smirnov test. Using MANOVA with post-hoc multiple comparison statistical analysis, brain metabolites were classified according to developmental changes and regional differences (Table 1). Significant differences between hippocampus, striatum, and cerebral cortex for each postnatal age group were found for Ins and GPC + PCho ($P < 0.01$). For most of the metabolites, the differences between locations became apparent on P14 or later. The highest level of significance ($P < 0.001$) for the concentration differences of metabolites between hippocampus, striatum, and cerebral cortex were found for Asp, Ins, NAA, PE, Tau, and GPC + PCho. A correlation analysis of metabolite concentration vs. postnatal age, shown in the far right column of Table 1, indi-

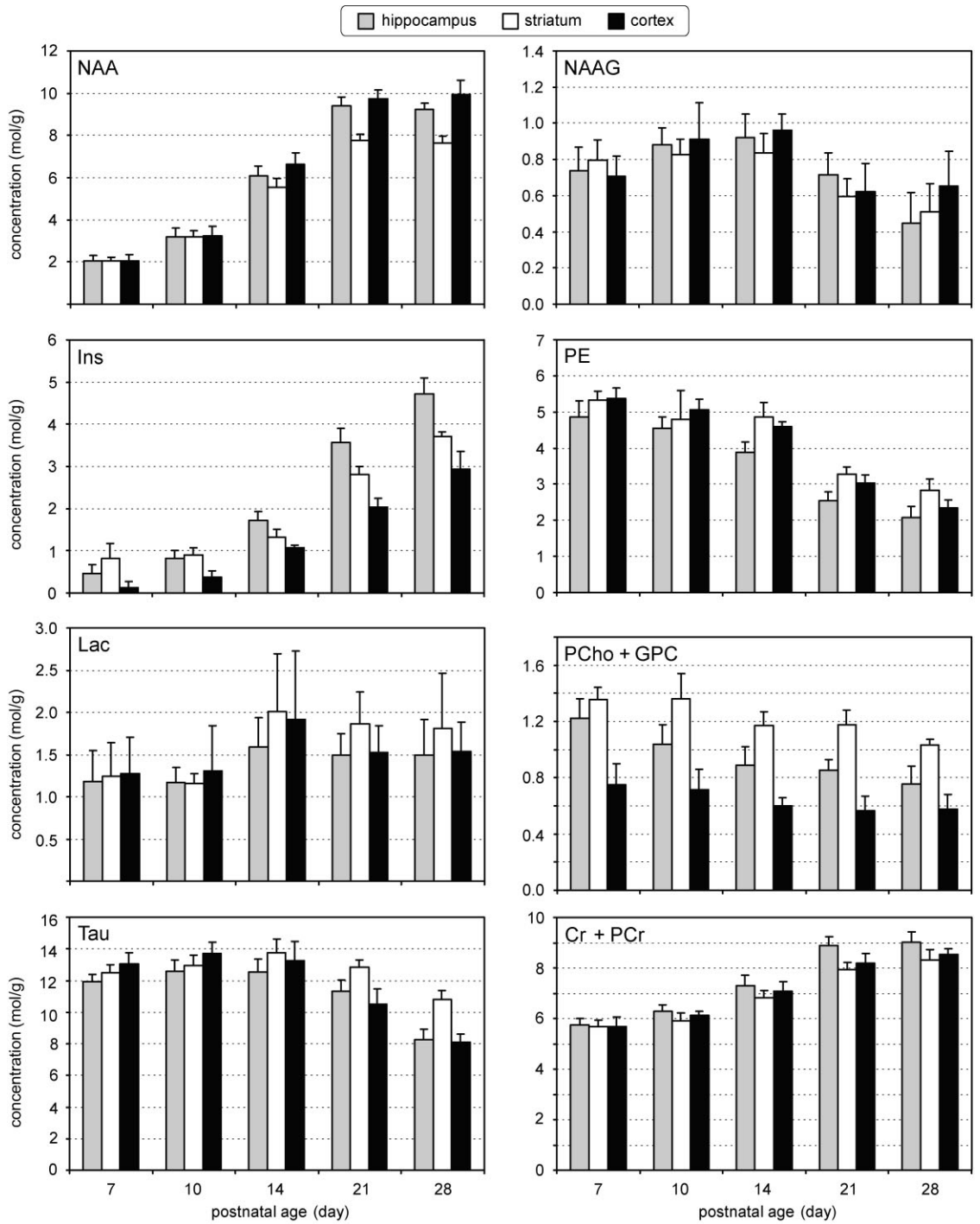

FIG. 6. Concentration of brain metabolites in hippocampus, striatum, and cerebral cortex in the developing rat brain (P7–P28). Error bars denote standard deviations (continuation of Fig. 5).

cated that metabolites with the highest rates of concentration increase (> 0.10 μmol g^{-1} day^{-1}) between P7 and P28 were Glu, Ins, NAA, and PCr + Cr. The most rapid decrease in concentration over time (> 0.10 μmol g^{-1} day^{-1}) was found for PE and Tau, whereas Asp, GABA, Glc, and GSH did not correlate with postnatal age ($P > 0.05$). However, Asp, GABA, NAAG, and Tau reached maximum concentration approximately on P14, as judged from the opposite signs of the correlation coefficients resulting from correlation analysis of the subsets of data (P7–P14 vs. P14–P28).

Interestingly, the ratios of [PCr]/[Cr] and [Glu]/[Gln] also peaked between P14 and P21. The ratio [PCr]/[Cr] rose from 0.5 ± 0.2 (P7) to a maximum of 1.0 ± 0.2 (P14–P21) and decreased to 0.8 ± 0.2 on day P28. The ratios of [Glu]/[Gln] changed within a range of 2.0–4.5 and significant differences in [Glu]/[Gln] were found between locations (Fig. 7).

Table 1
Schematic Representation of the Differences in Metabolite Concentrations Between Hippocampus, Striatum, and Cerebral Cortex and the Type of Concentration Changes During Postnatal Brain Development

Metabolite	Differences between locations[a]					Changes with age[b]
	P7	P10	P14	P21	P28	
Mac						↑
Ala						↑
Asp						
Cr						↑ ↑
PCr						↑ ↑
GABA						
Glc						
Gln						↑ ↑
Glu						↑ ↑ ↑
GSH						
Ins						↑ ↑ ↑
Lac						
NAA						↑ ↑ ↑
NAAG						↓
PE						↓ ↓ ↓
Tau						↓ ↓ ↓
GPC + PCho						↓
Cr + PCr						↑ ↑ ↑

$P < 0.05$ $P < 0.01$ $P < 0.001$

[a]Shaded areas demonstrate differences in metabolite concentration between brain location (hippocampus, striatum, cerebral cortex) at three significance levels.

[b]Arrows indicate significant concentration increase (μmol g^{-1}day^{-1}): ↑ < 0.05, ↑ ↑ 0.05–0.10, ↑ ↑ ↑ > 0.10; or significant concentration decrease (μmol g^{-1} day^{-1}): ↓ < 0.05, ↓ ↓ 0.05–0.10, ↓ ↓ ↓ > 0.10; during brain development.

DISCUSSION

This study demonstrates that the postnatal development of the rat brain can be measured longitudinally with high reliability and reproducibility, indicating that very small changes in the neurochemical profile can be detected. The accuracy and reliability of metabolite concentrations quantified from in vivo ^{1}H NMR spectra can be judged from Cramer-Rao lower bounds provided by LCModel analysis. The consistently low values of the CRLB (less than 20%) for most of the metabolites included in the LCModel database for all brain regions and age groups guaranteed high reliability of quantified concentrations. For example, strongly represented metabolites, such as Tau and Cr + PCr, were quantified with CRLB $\leq$ 5% from all 114 processed spectra. The interindividual coefficient of variation (CV) was below 5% for total Cr and well below 10% for most metabolites (indicated by the error bars in Figs. 5, 6, representing SD). The similarity of the CRLB and CV implied that the variation between animals, including water signal referencing, did not contribute significantly to the variation of metabolite concentrations. Such a high reproducibility of the data, untypical for in vivo NMR spectroscopy, was attributed to a number of factors: First, the advantages of increased sensitivity and spectral resolution at 9.4 T were used to measure the neurochemical profiles in three different locations of the developing rat brain. However, the strength of the magnetic field alone was not sufficient to achieve this goal. Extremely powerful, custom-designed second-order shim coils (~0.04 mT/cm^2), manufactured by Magnex Scientific according to our specifications, were used. The shim system was strong enough to correct for second-order field inhomogeneities in measured brain regions of P7 rat pups, where the overall demand was highest and typically required 50–70% of available shim strength. Automatic shim adjustment by FASTMAP (16) ensured a high spectral resolution (water signal linewidth 8–12 Hz), which routinely resulted in resolved signals of the methylene groups of Cr and PCr (Figs. 2, 4). In addition, highly efficient water suppression achieved with the VAPOR technique (17), excellent localization performance of the sequence (STEAM combined with OVS) (17), and minimization of the chemical shift displacement error by using very strong slice selection gradients further guaranteed high reproducibility of spectra for the entire ^{1}H chemical shift range. Finally, the ultra-short echo-time of only 2 ms substantially minimized J-modulation of the coupled spin systems and signal attenuation caused by T_2 relaxation, which simplified the quantification of brain metabolites and eliminated effects of a potential variation of T_2 on metabolite quantification.

For several metabolites, such as Glu, Ins, Lac, NAA, and Tau (shown in Fig. 4), characteristic spectral patterns were easily discernible in all in vivo spectra (Fig. 2). Developmental changes in concentrations of several metabolites, such as NAA, Ins, Tau, Glu, PE, and total Cr, were evident from a visual inspection of the ^{1}H NMR spectra (Fig. 2). Concentration changes of weakly represented metabolites, such as GABA or Gln, were not as obvious; however, they can be estimated taking into account contributions of overlapping resonances in specific spectral regions. For example, only limited developmental concentration changes of GABA can be expected by inspection of the signal intensity at 2.28 ppm (Fig. 2), taking into account the signal contribution from macromolecules. Similarly, the signal intensity at 2.44 ppm (Fig. 2) indicates only a moderate increase in Gln concentration during postnatal brain development, taking into account the signal overlap of H-4 of Gln with one of the geminal CH_2 protons of NAA at 2.49 ppm. However, a precise quantification requires sophisticated fitting analysis, such as LCModel, even at 9.4 T. An example of LCModel spectral analysis is illustrated in Fig. 4, which shows contributions of the characteristic spectra of each individual metabolite included in the database.

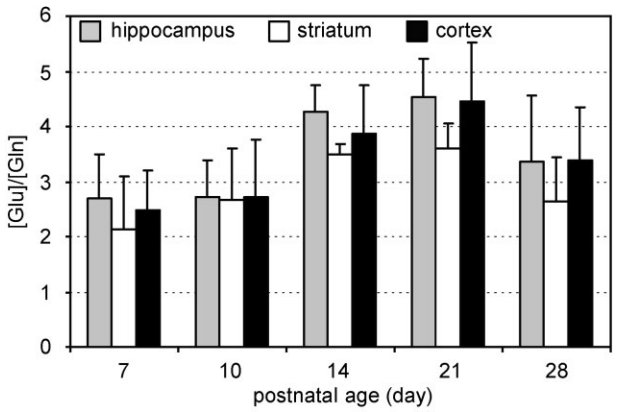

FIG. 7. Developmental changes of the glutamate/glutamine ratio in hippocampus, striatum, and cerebral cortex.

Table 2
Comparison of the Measured Metabolite Concentrations in Developing Rat Brain With the Literature Data

Metabolite	P7		P28		Reference
	This study[a]	Literature	This study[a]	Literature	
Asp	1.0–1.3	2.0–2.5	1.2–2.4	2.5–3.8	8,24
GABA	0.7–1.0	1.1–1.3	0.9–1.1	1.3–1.7	8,24
Gln	1.3–1.7	3.0–4.3	2.8–3.5	3.8–4.7	8,24
Glu	3.2–3.5	5.8–6.5	8.7–11.2	9.0–9.5	8,24
NAA	0.7–0.8	1.5–2.5	7.6–10.0	4.7–9.0	9,11
PE	4.9–5.4	3.6–8.0	2.1–2.8	1.7–4.0	11,24
Tau	12.0–13.0	12.0–13.0	8.1–10.8	5.0–7.4	24–27
Cr + PCr	5.7	5.2–6.5	8.3–9.0	8.5–9.7	11

Concentrations are expressed in units μmol/g.
[a]Ranges of averaged concentrations from hippocampus, striatum, and cerebral cortex.

The majority of the observed developmental *changes* of the neurochemical profile of the rat brain (Figs. 5, 6, Table 1), specifically the increase of NAA, Glu, Gln, and total Cr, as well as the decrease of PCho + GPC, PE, and Tau, are in agreement with previously published data of brain extracts (6–11,13,24,25). Minor developmental changes in concentrations observed for GABA and NAAG are also in agreement with previously published data (8,9).

Unfortunately, a survey of published metabolite concentrations in the developing rat brain indicates a rather broad range (8–14,24–28). Interestingly, the results of classic biochemical assays published by different laboratories more than two decades ago show a close agreement to within 10% (8,9,24–27). Therefore, we compared our in vivo data to the in vitro data published in the aforementioned articles. Absolute metabolite concentrations (in μmol/g) presented in Figs. 5 and 6 were in very good agreement with the in vitro data (Table 2). For example, the concentration of Tau in hippocampus, striatum, and cortex of a 7-day-old rat ranged in our study between 12–13 μmol/g, which is identical to the range of data published by several different laboratories (24–27). Small differences for some of the other metabolites can be explained by regional variation in the neurochemical composition of the brain tissues (28) as well as the effects of the catabolic reactions of metabolites in biochemical in vitro assays. Further, paired studies comparing metabolite concentrations in specific brain regions measured by in vivo NMR and by the analysis of brain extract analysis are needed to determine to what extent the regional variation, postmortem processes, or inaccuracies of the methods used can account for the differences.

Significant differences between hippocampus, striatum, and cerebral cortex were found for most of the metabolites (Table 1). Specific patterns of regional differences in metabolite concentrations were consistently detected during postnatal brain maturation, especially for P14, P21, and P28. Examples of regional differences include Glu being highest in cortex, NAA lowest in striatum, Ins highest in hippocampus, and the choline compounds highest in striatum. This resulted in a characteristic neurochemical profile for each studied brain region that cannot be explained either by regional differences in gray/white matter ratios or by differences in water content, which was used as internal reference for quantification. For most compounds, regional differentiation started on postnatal day P14 (summarized in Table 2), coinciding with the period (P10–P17) of active brain growth, myelination, and rapid increase in cerebral energy metabolism (29). These, in turn, are associated with the acquisition of the specific brain functions, such as audition (P10–P14) and vision and locomotion (P14–P17) (30). The observed differences in neurochemical profiles between locations are not surprising, considering the variable populations of different neural cell types characterized by the specific chemical composition (31). To what extent regional differences in metabolism also contributed to the different neurochemical profiles remains to be determined. Changes of Glc and Lac were not interpreted, because their concentrations can depend on the anesthesia regimen, which is outside of the scope of the current study.

The 2-fold increase in [PCr]/[Cr] ratio during postnatal brain development (P7–P21) coincided with the 4-fold increase in creatine kinase activity between P12 and P17 (32). The ratio of [Glu]/[Gln] depended on location and age (Fig. 7) and interestingly peaked between P14 and P21. The [Glu]/[Gln] ratio in normal brain is an important parameter, because Glu and Gln metabolism in the brain is closely related to neurotransmission and Glu and Gln cycling between neurons and glia (33,34). In addition, the decrease in [Glu]/[Gln] ratio from a normal value for a specific brain region and age is assumed to be a marker of a metabolic defect (35,36).

The in vivo measurement of the neurochemical profile using NMR spectroscopy has several advantages, such as elimination of effects related to animal termination and brain extraction and the possibility of a longitudinal experimental design resulting in substantial reduction of required animals. Previously, only a limited number of metabolites (NAA, Cho, total Cr, PCr, PE) have been measured in developing rat brain using either in vivo ^{1}H or ^{31}P NMR spectroscopy (12–14). In the present study, several metabolites key to brain development (e.g., PE and PCr), until now only accessible in ^{31}P NMR spectra, were detected and quantified using ^{1}H NMR spectroscopy. The excellent agreement of our data with the results of brain extract analysis indicated that at least 16 metabolites can be reliably quantified with high accuracy and precision in specific regions of the developing rat brain using in vivo ^{1}H NMR spectroscopy at 9.4 T.

We conclude that in vivo ^{1}H NMR spectroscopy at high magnetic fields, based on powerful shimming, efficient

water suppression, high-performance localization pulse sequence, and LCModel fitting can accurately measure the neurochemical profile in specific regions of the developing rat brain. Because the current study design was longitudinal and completely noninvasive, this approach can be extended to study human brain development taking into account the availability of whole-body 7 T systems (37). Given the wide variability in rates of regional brain growth and the differential vulnerability of brain regions to metabolic insults early in life (19,20), such detailed neurochemical information is likely to provide new insight into the neurochemical processes of normal and pathologic brain development and to monitor the response to therapies.

REFERENCES

1. Mukherjee P, Miller JH, Shimony JS, Conturo TE, Lee BC, Almli CR, McKinstry RC. Normal brain maturation during childhood: developmental trends characterized with diffusion-tensor MR imaging. Radiology 2001;221:349–358.
2. Martin E, Marcar VL. Functional MR imaging in pediatrics. Magn Reson Imag Clin N Am 2001;9:231–246.
3. Huppi PS. MR imaging and spectroscopy of brain development. Magn Reson Imag Clin N Am 2001;9:1–17.
4. Dobbing J. Vulnerable periods in developing brain. In: Dobbing J, editor. Brain, behaviour, and iron in the infant diet. New York: Springer; 1990. p 1–25.
5. McIlwain H, Bachelard HS. Biochemistry and the central nervous system, 5th ed. Edinburgh: Churchill Livingstone; 1985. p 371–412.
6. Sturman JA, Rassin DK, Gaull GE. Taurine in development. Life Sci 1977;21:1–22.
7. Corbett RJ. In vivo multinuclear magnetic resonance spectroscopy investigations of cerebral development and metabolic encephalopathy using neonatal animal models. Semin Perinatol 1990;14:258–271.
8. Bayer SM, McMurray WC. The metabolism of amino acids in developing rat brain. J Neurochem 1967;14:695–706.
9. Koller KJ, Coyle JT. Ontogenesis of N-acetyl-aspartate and N-acetyl-aspartyl-glutamate in rat brain. Brain Res 1984;317:137–140.
10. Bates TE, Williams SR, Gadian DG, Bell JD, Small RK, Iles RA. 1H NMR study of cerebral development in the rat. NMR Biomed 1989;2:225–229.
11. Burri R, Bigler P, Straehl P, Posse S, Colombo JP, Herschkowitz N. Brain development: 1H magnetic resonance spectroscopy of rat brain extracts compared with chromatographic methods. Neurochem Res 1990;15:1009–1016.
12. Tofts P, Wray S. Changes in brain phosphorus metabolites during the post-natal development of the rat. J Physiol 1985;359:417–429.
13. Burri R, Lazeyras F, Aue WP, Straehl P, Bigler P, Althaus U, Herschkowitz N. Correlation between 31P NMR phosphomonoester and biochemically determined phosphorylethanolamine and phosphatidylethanolamine during development of the rat brain. Dev Neurosci 1988;10:213–221.
14. Hida K, Kwee IL, Nakada T. In vivo 1H and 31P NMR spectroscopy of the developing rat brain. Magn Reson Med 1992;23:31–36.
15. Gruetter R. Automatic, localized in vivo adjustment of all first- and second-order shim coils. Magn Reson Med 1993;29:804–811.
16. Gruetter R, Tkáč I. Field mapping without reference scan using asymmetric echo-planar techniques. Magn Reson Med 2000;43:319–323.
17. Tkáč I, Starčuk Z, Choi IY, Gruetter R. In vivo 1H NMR spectroscopy of rat brain at 1 ms echo time. Magn Reson Med 1999;41:649–656.
18. Pfeuffer J, Tkáč I, Provencher SW, Gruetter R. Toward an in vivo neurochemical profile: quantification of 18 metabolites in short-echo-time (1)H NMR spectra of the rat brain. J Magn Reson 1999;141:104–120.
19. Nelson C, Silverstein FS. Acute disruption of cytochrome oxidase activity in brain in a perinatal rat stroke model. Pediatr Res 1994;36:12–19.
20. de Ungria M, Rao R, Wobken JD, Luciana M, Nelson CA, Georgieff MK. Perinatal iron deficiency decreases cytochrome c oxidase (CytOx) activity in selected regions of neonatal rat brain. Pediatr Res 2000;48:169–176.
21. Klose U. In vivo proton spectroscopy in presence of eddy currents. Magn Reson Med 1990;14:26–30.
22. Provencher SW. Estimation of metabolite concentrations from localized in vivo proton NMR spectra. Magn Reson Med 1993;30:672–679.
23. De Souza SW, Dobbing J. Cerebral edema in developing brain. I. Normal water and cation content in developing rat brain and postmortem changes. Exp Neurol 1971;32:431–438.
24. Oja SS, Uusitalo AJ, Vahvelainen ML, Piha RS. Changes in cerebral and hepatic amino acids in the rat and guinea pig during development. Brain Res 1968;11:655–661.
25. Agrawal HC, Davison AN, Kaczmarek LK. Subcellular distribution of taurine and cysteinesulphinate decarboxylase in developing rat brain. Biochem J 1971;122:759–763.
26. Oja SS, Piha RS. Changes in the concentration of free amino acids in the rat brain during postnatal development. Life Sci 1966;5:865–870.
27. Sturman JA, Rassin DK, Gaull GE. Taurine in developing rat brain: maternal-fetal transfer of [35 S] taurine and its fate in the neonate. J Neurochem 1977;28:31–39.
28. Florian CL, Williams SR, Bhakoo KK, Noble MD. Regional and developmental variations in metabolite concentration in the rat brain and eye: a study using 1H NMR spectroscopy and high performance liquid chromatography. Neurochem Res 1996;21:1065–1074.
29. Rice D, Barone S Jr. Critical periods of vulnerability for the developing nervous system: evidence from humans and animal models. Environ Health Perspect 2000;108 Suppl 3:511–533.
30. Nehlig A. Cerebral energy metabolism, glucose transport and blood flow: changes with maturation and adaptation to hypoglycaemia. Diabetes Metab 1997;23:18–29.
31. Urenjak J, Williams SR, Gadian DG, Noble M. Proton nuclear magnetic resonance spectroscopy unambiguously identifies different neural cell types. J Neurosci 1993;13:981–989.
32. Holtzman D, Tsuji M, Wallimann T, Hemmer W. Functional maturation of creatine kinase in rat brain. Dev Neurosci 1993;15:261–270.
33. Gruetter R, Seaquist ER, Kim S, Ugurbil K. Localized in vivo 13C-NMR of glutamate metabolism in the human brain: initial results at 4 tesla. Dev Neurosci 1998;20:380–388.
34. Sibson NR, Dhankhar A, Mason GF, Rothman DL, Behar KL, Shulman RG. Stoichiometric coupling of brain glucose metabolism and glutamatergic neuronal activity. Proc Natl Acad Sci USA 1998;95:316–321.
35. Jenkins BG, Klivenyi P, Kustermann E, Andreassen OA, Ferrante RJ, Rosen BR, Beal MF. Nonlinear decrease over time in N-acetyl aspartate levels in the absence of neuronal loss and increases in glutamine and glucose in transgenic Huntington's disease mice. J Neurochem 2000;74:2108–2119.
36. Tkáč I, Keene CD, Pfeuffer J, Low WC, Gruetter R. Metabolic changes in quinolinic acid-lesioned rat striatum detected noninvasively by in vivo (1)H NMR spectroscopy. J Neurosci Res 2001;66:891–898.
37. Tkáč I, Andersen P, Adriany G, Merkle H, Ugurbil K, Gruetter R. In vivo (1)H NMR spectroscopy of the human brain at 7 T. Magn Reson Med 2001;46:451–456.